The Double-Stranded RNA Bluetongue Virus Induces Type I Interferon in Plasmacytoid Dendritic Cells via a MYD88-Dependent TLR7/8-Independent Signaling Pathway

JVI Journals.ASM.org

The Double-Stranded RNA Bluetongue Virus Induces Type I Interferon in Plasmacytoid Dendritic Cells via a MYD88-Dependent TLR7/8-Independent Signaling Pathway

Suzana Ruscanu,[a] Florentina Pascale,[a,b] Mickael Bourge,[c] Behzad Hemati,[a]* Jamila Elhmouzi-Younes,[a] Céline Urien,[a] Michel Bonneau,[b] Haru Takamatsu,[d] Jayne Hope,[e] Peter Mertens,[d] Gilles Meyer,[f] Meredith Stewart,[g] Polly Roy,[g] Eliane F. Meurs,[h] Stéphanie Dabo,[h] Stéphan Zientara,[i] Emmanuel Breard,[i] Corinne Sailleau,[i] Emilie Chauveau,[i] Damien Vitour,[i] Bernard Charley,[a] and Isabelle Schwartz-Cornil[a]

Virologie et Immunologie Moléculaires, UR892 INRA, Jouy-en-Josas, France[a]; Centre de Recherche en Imagerie Interventionnelle, Institut National de la Recherche Agronomique, Jouy-en-Josas, France[b]; IFR87 La Plante et son Environnement, IMAGIF CNRS, Gif sur Yvette, France[c]; Vector Bourne Viral Disease Programme, Institute for Animal Health, Woking, Surrey, United Kingdom[d]; Roslin Institute, University of Edinburgh, Easter Bush, Midlothian, United Kingdom[e]; Université de Toulouse, INP, ENVT, INRA UMR1225, IHAP, Toulouse, France[f]; London School of Hygiene and Tropical Medicine, London, United Kingdom[g]; Institut Pasteur, Hepacivirus and Innate Immunity, Paris, France[h]; and UMR 1161 ANSES/INRA/ENVA, Maisons-Alfort, France[i]

Dendritic cells (DCs), especially plasmacytoid DCs (pDCs), produce large amounts of alpha/beta interferon (IFN-α/β) upon infection with DNA or RNA viruses, which has impacts on the physiopathology of the viral infections and on the quality of the adaptive immunity. However, little is known about the IFN-α/β production by DCs during infections by double-stranded RNA (dsRNA) viruses. We present here novel information about the production of IFN-α/β induced by bluetongue virus (BTV), a vector-borne dsRNA *Orbivirus* of ruminants, in sheep primary DCs. We found that BTV induced IFN-α/β in skin lymph and in blood *in vivo*. Although BTV replicated in a substantial fraction of the conventional DCs (cDCs) and pDCs *in vitro*, only pDCs responded to BTV by producing a significant amount of IFN-α/β. BTV replication in pDCs was not mandatory for IFN-α/β production since it was still induced by UV-inactivated BTV (UV-BTV). Other inflammatory cytokines, including tumor necrosis factor alpha (TNF-α), interleukin-6 (IL-6), and IL-12p40, were also induced by UV-BTV in primary pDCs. The induction of IFN-α/β required endo-/lysosomal acidification and maturation. However, despite being an RNA virus, UV-BTV did not signal through Toll-like receptor 7 (TLR7) for IFN-α/β induction. In contrast, pathways involving the MyD88 adaptor and kinases dsRNA-activated protein kinase (PKR) and stress-activated protein kinase (SAPK)/Jun N-terminal protein kinase (JNK) were implicated. This work highlights the importance of pDCs for the production of innate immunity cytokines induced by a dsRNA virus, and it shows that a dsRNA virus can induce IFN-α/β in pDCs via a novel TLR-independent and Myd88-dependent pathway. These findings have implications for the design of efficient vaccines against dsRNA viruses.

The *Reoviridae* are a family of nonenveloped double-stranded RNA (dsRNA) viruses that include reoviruses of clinical importance, such as rotaviruses in humans and orbiviruses in animals. In many instances, the diseases induced by the reoviruses are acute, showing high prevalence with variable degrees of severity and mortality in immunologically naive populations. Among the orbiviruses, bluetongue virus (BTV), which primarily infects ruminants, recently caused major outbreaks in many European countries and induced large economic losses due to direct animal disease and death, loss of productivity, restrictions on trade and animal movements, and expensive surveillance and vaccination campaigns (58). There are 26 distinct BTV serotypes (BTV1 to BTV26) that induce serotype non-cross-protective immunity and that have an impact on vaccination strategies.

The innate immune responses elicited by the dsRNA viruses, including the production of type I interferon (alpha/beta interferon [IFN-α/β]) and other inflammatory cytokines, are likely to be key factors in the expression of their variable pathogenicity levels (34). Different dsRNA sensors and signaling pathways have been described that mediate the production of innate cytokines in response to reovirus infections, including (i) the TLR3 (Toll-like receptor 3)-TRIF (TIR [Toll–IL-1 {interleukin-1} resistance] domain-containing adaptor inducing IFN-β) endosomal pathway (1), (ii) the RIG-I (retinoid acid-inducible gene I) or MDA5 (melanoma differentiation-associated gene 5)-MAVS (mitochondrial antiviral signaling) mitochondrial pathway (6, 60, 68), (iii) the PKR (dsRNA-activated protein kinase) pathway (18, 19, 60), and (iv) the newly described TRIF-dependent DexD/H-box helicases (69). These signaling pathways are involved in innate responses to dsRNA virus in cell types such as fibroblasts, epithelial cells, and conventional dendritic cells (cDCs). They also seem to be alternatively used for sensing and signaling depending on the cell type and on the subcellular compartment where they encounter the dsRNA (6, 60, 69).

Although both hematopoietic and nonhematopoietic cells are thought to be involved in the innate cytokine responses to dsRNA

Received 2 November 2011 Accepted 2 March 2012
Published ahead of print 21 March 2012
Address correspondence to Isabelle Schwartz-Cornil, isabelle.schwartz@jouy.inra.fr.
* Present address: Animal Science Department, Karaj Branch, Islamic Azad University, Karaj, Iran.
Supplemental material for this article may be found at http://jvi.asm.org/.

doi:10.1128/JVI.06716-11

viruses *in vivo*, the use of hematopoietic mouse chimeras revealed that hematopoietic cells, including both cDCs and plasmacytoid DCs (pDC), play a key role in type I IFN production during orthoreovirus infection (34). Indeed, PDCs are the main hematopoietic cell type specialized in the production of innate cytokines and, especially, of huge amounts of IFN-α/β. PDC responses to viral triggers were studied in single-stranded RNA (ssRNA) and DNA virus infections. TLR7 and TLR9 linked to the MyD88 adaptor molecule were demonstrated to be the major and possibly the only innate receptors that activate this cell type. However, cytosolic DexD/H-box helicases linked to MyD88 can also be involved in viral DNA recognition in pDCs (36). Both orthoreovirus infection in mice and rotavirus infection in human are capable of triggering the production of IFN-α/β in pDCs. However, as pDCs do not express TLR3 (14, 48) and do not use the RIG-1/MDA5 signaling pathway (35, 54, 63), it is still not known how pDCs respond to dsRNA virus infection. In addition, very few studies have been reported to date concerning the relative contribution of pDCs to innate cytokine production in response to dsRNA virus infection.

In this study, we addressed the role of pDCs in IFN-α/β production in response to BTV compared to the role of other hematopoietic cells, including the cDCs that represent the initial cell target for BTV replication after its injection into sheep skin. In sheep, pDCs are rare cells found in blood (<0.5%), and they also circulate in skin lymph (52). Preliminary experiments in C57BL/6 mice indicated that murine hematopoietic cells and purified murine pDCs do not respond to BTV by producing IFN-α/β, preventing the use of mouse models to address BTV signaling for IFN-α/β production. We therefore directly investigated the interaction of BTV with its natural sheep host pDCs and cDCs, and we were able to use primary cells, due to the large quantities of cells that can be collected in this species.

MATERIALS AND METHODS

Medium and reagents. X-Vivo 15 (BioWhittaker) supplemented with 1% heat-inactivated fetal calf serum (FCS), 100 IU/ml penicillin, and 100 μg/ml streptomycin was used as the cell culture medium for sheep cells. RPMI 1640 supplemented with 4% horse serum (HS) was used for cell immunolabeling (fluorescence-activated cell sorting [FACS] medium). Dulbecco's modified Eagle's medium (DMEM) supplemented with 10% FCS, 100 IU/ml penicillin, and 100 μg/ml streptomycin was used for baby hamster kidney-21 (BHK21) culture (virus growth and titration). Eagle's minimum essential medium (EMEM) supplemented with 5% FCS, 1.5 mM L-glutamine, 100 IU/ml penicillin, and 100 μg/ml streptomycin was used for Madin-Darby bovine kidney (MDBK) cell culture. CpG-A D32-oligodeoxynucleotide with the sequence ggT GCG TCG ACG CAG ggg gg (lowercase letters for phosphothioate linkages and uppercase letters for phosphodiester linkages) was produced by BioSource International. Opti-MEM (Invitrogen) and Lipofectamine 2000 (Invitrogen) were used for poly(I·C) (Sigma-Aldrich) transfection. 2-Aminopurine (2-AP), chloroquine, and bafilomycin A1 were obtained from Sigma-Aldrich. SP600125 (Jun N-terminal protein kinase [JNK] inhibitor) and PKR inhibitor (C16) were from Calbiochem (Merck), and PD184352 was from AXON Medchem. The MyD88 homodimerization inhibitory peptide set was purchased from Imgenex. The A151 oligonucleotide [$(TTAGGG)_4$], a TLR7/9 antagonist (26), was synthesized at the Pasteur Institute Genopole, Paris, France.

Virus preparations. Wild-type field strains of BTV serotypes 1, 2, and 8 (BTV1, BTV2, and BTV8) were isolated in France in 2007, 2001 (Corsica), and 2006, respectively. These viruses are still virulent and pathogenic in sheep. The modified live attenuated vaccine strain BTV2 (a-BTV2) was produced by Onderstepoort Biological Products in the Republic of South Africa. For purified BTV1, virus particles of the South African reference strain of BTV1 were purified on sucrose gradients as previously described by Mertens et al. (46). This strain of BTV is held in the Institute for Animal Health (IAH, United Kingdom) reference collection (www.reoviridae.org/dsRNA_virus_proteins/ReoID/btv-1.htm) and is identified by strain number RSArrrr/01.

Viruses were grown on BHK21 cells. For preparation of crude viral stocks, confluent BHK21 cell layers were infected with 0.1 50% tissue culture infective dose ($TCID_{50}$)/cell and cells were incubated at 37°C and 5% CO_2. When cytopathic effect was complete (4 to 5 days), culture supernatants were aliquoted and stored at −80°C. The $TCID_{50}$ values were estimated by the method of Spearman-Karber using a previously described protocol (27).

Heat inactivation of BTV was done at 56°C for 30 min. For UV inactivation, virus preparations (2 ml) were exposed to 254-nm UV at a 10-cm distance from the source in 35-mm-diameter dishes. Virus was completely inactivated (UV-BTV) in 20 min when the dose of UV was 2.3 J/cm^2 (see Fig. S2 in the supplemental material). Formol-inactivated influenza virus (PR8/34) was prepared as previously described (61).

Animals and afferent lymph and blood collection. Prealpe BTV-seronegative female sheep, originating from l'Unité Commune d'Expérimentation Animale in Jouy-en-Josas, France, were cannulated at the Centre de Recherche en Imagerie Interventionnelle in Jouy-en-Josas as previously described (23). Low-molecular-weight heparin (enoxaparin [Lovenox], Sanofi-Aventis) was injected intradermally into the shoulder skin every 12 h (2,000 IU anti-enoxaparin per injection). Lymph was collected twice a day in flasks containing 500 IU heparin, 10,000 IU penicillin, and 10 mg streptomycin. This protocol was carried out in strict accordance with the recommendations of the Charte Nationale Portant sur l'Éthique en Expérimentation Animale established by the Comité National de Réflexion Éthique sur l'Expérimentation Animale (CNREEA, Ministère de l'Enseignement Supérieur et de la Recherche et Ministère de l'Agriculture et de la Pêche) and was approved by the Committee on the Ethics of Animal Experiments of the INRA research center in Jouy-en-Josas and AgroParisTech under the number 11-019. The animal experiments were carried out under licenses issued by the Veterinary Services of Versailles (accreditation numbers A78-93, A78-15, and A78-730).

Blood was collected from Prealpe sheep (1 to 4 years old) by venous puncture on sodium citrate.

***In vivo* infections.** Two cannulated sheep were inoculated intradermally with 10^5 $TCID_{50}$ a-BTV2 and BTV8, respectively, in the biosafety level 3 (BSL3) animal facilities of the Centre de Recherche en Biologie Médicale in Maisons-Alfort, France. Lymph draining the corresponding area of the skin was harvested at different time points as indicated below, and the sheep were terminated at the end of the experiment.

For IFN-α/β detection in sera, BTV-seronegative Prealpe sheep were infected subcutaneously and intravenously with, respectively, 1 and 5 ml of blood from a viremic BTV8-infected animal (8.1×10^6 BTV RNA copies/ml) in the BSL3 facilities of the Plate-Forme d'Infectiologie Expérimentale in Nouzilly, France. Sera were obtained from the infected animals at 0, 2, 6, and 10 days after infection. The sheep were terminated at the end of the experiment.

Low density (LD) lymph and LD peripheral blood mononuclear cell (PBMC) isolations. Total afferent lymph cells were spun down at $700 \times g$, and LD lymph cells were obtained after centrifugation on a 1.065-g/ml iodixanol density gradient (OptiPrep, Nycomed Pharma) as previously described (57).

PBMCs were obtained from sheep peripheral blood buffy coat samples by 1.076-g/ml Percoll (GE Healthcare) density gradient centrifugation (8). LD PBMCs were obtained after centrifugation on iodixanol gradient as described for lymph cells.

***In vitro* activation of LD lymph cells, LD PBMCs, cDCs, and pDCs with BTV and IFN-α/β inducers and use of inhibitors.** LD lymph cells, LD PBMCs, and pDCs were incubated at 37°C with 0.01 to 0.5 $TCID_{50}$ BTV/cell in cell culture medium. The cell and viral concentrations used in

each experiment are specified in the text and/or in the figure legends. Generally a 0.06 $TCID_{50}$ BTV/cell concentration was used with BTV8 and lower concentrations were used when viral strain stocks were at lower titers. For testing IFN-α/β production in supernatants, cells were cultured overnight with BTV. For detection of intracellular NS2 and surface CD80/86 expression, cells were cultured for 48 h with BTV. For detection of viral replication in pDCs by quantitative reverse transcriptase PCR (qRT-PCR), FACS-sorted pDCs were incubated with 0.06 $TCID_{50}$ BTV8/cell for 1 h at 37°C, washed carefully four times in culture medium to remove unbound virus, and lysed either right away or after 48 h of culture for RNA extraction.

CpG-A was added at a 10-μg/ml final concentration. Poly(I·C) (1 μg/ml) was transfected using Lipofectamine 2000 as previously described (30), by mixing 200 ng poly(C) with 1 μl Lipofectamine 2000 that was added to the 200-μl/well culture. Formol-inactivated influenzavirus (PR8/34) was used at a 4-μg/ml dose. Chloroquine, bafilomycin A1, A151, C16, JNK, and ERK (extracellular signal-regulated kinase) inhibitors were added to cells 30 min before stimulation, and cells were incubated overnight after adding the activators. MyD88 inhibitory and control peptides were incubated overnight with LD PBMCs. Thereafter, cells were stimulated with CpG-A (10 μg/ml) and UV-BTV8 (0.06 $TCID_{50}$/cell) for 12 h. After the stimulation period, cell supernatants were collected and kept at −20°C until IFN-α/β measurement.

Immunolabeling of cell subsets for analysis and/or sorting. Lymph cDCs were isolated from LD lymph cells by positive immunomagnetic cell sorting (Myltenyi Biotech) as previously described using an anti-CD11c primary antibody (27). Lymph pDCs were selected from LD lymph cells using immunomagnetic cell selection as described before (52). For pDC staining and/or sorting by flow cytometry, LD PBMCs were saturated for 20 min on ice in FACS medium and surface staining was performed using primary antibodies (2 μg/ml) against B cells (DU2-104 clone, IgM), CD8 cells (7C2 clone, IgG2a), TCRγ/δ (T cell receptor gamma/delta) cells (CC15 clone, IgG2a), CD11b cells (ILA-130 clone, IgG2a), CD11c cells (BAQ153A clone, IgM), and CD45RB cells (CC76 clone IgG1). After washing, cells were incubated with cyanin 5 or phycoerythrin (PE)-conjugated goat anti-mouse isotype-specific antibodies (Caltag) for 20 min on ice. Cells were washed in FACS medium and resuspended in Hanks' balanced salt solution (HBSS) plus 1% heat-inactivated FCS for cytometry sorting or in phosphate-buffered saline (PBS) for FACS analysis. Blood pDCs were sorted as B^- $CD8^-$ $CD11b^-$ $TCR\gamma/\delta^-$ $CD11c^-$ $CD45RB^+$ FSC^{high} cells based on their capacity to produce IFN-α/β upon CpG-A stimulation (see Fig. S1 in the supplemental material).

For staining with two monoclonal antibodies (MAbs) of the same isotype (IgG1) that needed to be distinguished (i.e., costaining of cDCs and pDCs and CD80/CD86 labeling on pDCs), LD PBMCs were first labeled at 4°C with the anti-CD45RB IgG1 MAb (2 μg/ml), followed by a saturating concentration (50 μg/ml) of fluorescein isothiocyanate (FITC)-donkey Fab anti-mouse IgG (Jackson ImmunoResearch). After two washes in FACS medium, cells were incubated with the second IgG1 primary MAb (i.e., anti-CD11c [OM1 clone] or anti-CD80 [ILA-159 clone] plus anti-CD86 [ILA-190 clone]) and with the anti-B (DU2-104 clone, IgM), anti-CD8 (7C2 clone, IgG2a), anti-TCRγ/δ (CC15 clone, IgG2a), anti-CD11b (ILA-130 clone, IgG2a), and anti-CD11c (BAQ153A clone, IgM). These primary antibodies were detected with PE-conjugated goat anti-mouse IgG1 and Cy5-conjugated goat anti-mouse IgG2a or IgM (Molecular Probes). Blood cDCs were sorted from LD PBMCs as B^- $CD8^-$ $CD11b^-$ $TCR\gamma/\delta^-$ $CD45RB^-$ $CD11c^+$ FSC^{high} cells.

For NS2 detection in BTV-infected pDCs, cellular fixation and permeabilization were performed using the Fix & Perm Kit (Caltag) and intracellular NS2 was revealed with a rabbit serum against NS2 (1:500) as described previously (27).

Nonrelevant antibodies (IgG1, IgG2a, IgM, and rabbit nonimmune serum) were consistently used as controls to measure the level of nonspecific background signal caused by primary antibodies.

Cell viability was determined by staining nonviable cells with 7-amino actinomycin D (7-AAD; 2 μg/ml), and flow cytometry analysis was performed to measure the percentage of surviving (7-AAD-negative) cells.

The pDCs and cDCs (between 2×10^5 and 5×10^5 per 500 ml of blood collected) were sorted by flow cytometry on the ImaGif cytometry platform using the analyzer-sorter MoFlo XDP cytometer and the Summit 5.2 software from Beckman Coulter (purity of >98%). Due to the low number of purified pDC that could be obtained, only single experimental points could be done per sheep. The validity of the results was demonstrated by repeating these single experimental points using different sheep (see figure legends). The flow cytometry analysis of NS2 and CD80/86 expression in pDCs was done using a FACSCalibur cytometer (Becton Dickinson) with the CellQuest Pro and/or FlowJo software.

IFN-α/β detection (bioassay) and ruminant IFN-α ELISA. IFN-α/β in cell supernatants, lymph fluids or sera was quantified using a cytopathic reduction bioassay with MDBK cells challenged with vesicular stomatitis virus. An internal IFN-α reference was included as described elsewhere (52). Each supernatant was tested over eight serial dilutions. Data are expressed as IFN-α/β units per ml. A specific bovine/ovine IFN-α enzyme-linked immunosorbent assay (ELISA) was used as described previously using anti-bovine IFN-α 1C6 and 1D10 MAbs and rabbit anti-bovine IFN-α IgG (52).

Cytokine mRNA detection by qRT-PCR. Total RNA was extracted using the Arcturus PicoPure RNA isolation kit (Arcturus). To exclude DNA contamination, RNA samples were treated with RNase-free DNase (Qiagen). cDNA was prepared using SuperScript III RT (Invitrogen). Quantitative real-time PCR was done using 5 ng cDNA with 300 nM primers in a final reaction mixture volume of 25 μl 1× SYBR green PCR master mix (Applied Biosystems) using an Eppendorf Mastercycler ep realplex system.

The primers used were glyceraldehyde-3-phosphate dehydrogenase (GAPDH) (forward, CACCATCTTCCAGGAGCGAG, and reverse, CCA GCATCACCCCACTTGAT), IFN-α (forward, TCTGCAAGAGAAGGG ACACA, and reverse, CCTGCAAGTTTGTTGAGGAAG), tumor necrosis factor (TNF) (forward, CAAGGGCCAGGGTTCTTACC, and reverse, GCCCACCCATGTCAAGTTCT), IL-6 (forward, GCTGCTCCTGGTGA TGACTTC, and reverse, GGTGGTGTCATTTTTGAAATCTTCT), and IL-12 (forward, TCTCGGCAGGTGGAAGTCA, and reverse, ACTTTGG CTGAGGTTTGGTCTG). Quantitative analysis was performed using the Realplex software (Eppendorf). Cytokine mRNA levels relative to the amount of GAPDH were calculated by analyzing the cycle threshold (C_T) values for each amplification curve, and the arbitrary units were established by the formula $2^{-[CT(\text{target}) - CT(\text{GAPDH})]}$.

Viral RNA detection was done using a commercial pan-BTV real-time RT-PCR (Adiavet BTV real-time A352; Adiagene, France) targeting segment 10 of BTV, which is highly conserved among BTV serotypes.

Statistical analyses. Due to the low numbers of purified pDCs that could be collected from 500 ml of blood in many instances, replicates and statistics could not be done within an experiment, but the experiments were repeated with different animals. When replicates were possible, data were expressed as means ± standard errors of the means (SEM). Statistical significance of differences was determined by paired or unpaired Student's *t* tests, by a paired one-tail Wilcoxon test, or by a Kruskal-Wallis test. The test used is mentioned in the figure legends (in the figures, one asterisk shows a P value of <0.05 and two asterisks show a P value of <0.005). Differences were considered statistically significant for P values of <0.05. Statistical analyses were performed using GraphPad Prism 5 software.

RESULTS

Administration of BTV in sheep induces IFN-α/β in afferent skin lymph and in blood. We first examined whether BTV induces IFN-α/β *in vivo* in sheep. We took advantage of the possibility to sequentially collect afferent skin lymph in this species after virus inoculation in the skin (10, 27). Inoculation of attenuated BTV2 (a-BTV2) and wild-type BTV8 (BTV8) in the skin in-

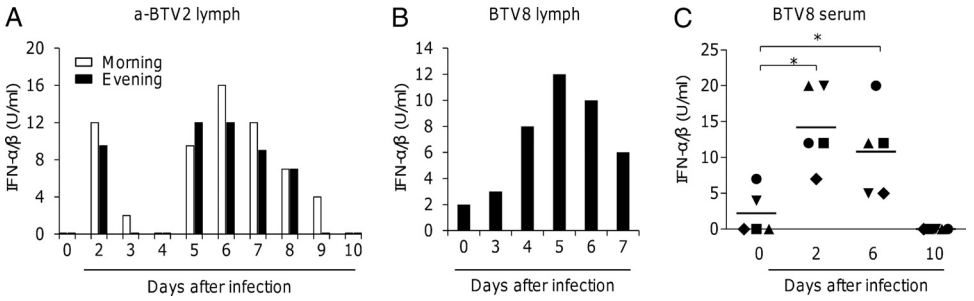

FIG 1 BTV induces IFN-α/β in afferent skin lymph (A and B) and in serum (C) *in vivo*. (A and B) Two cannulated sheep were inoculated intradermally with 10^5 $TCID_{50}$ a-BTV2 (A) and BTV8 (B), respectively. Afferent lymph was collected sequentially, and IFN-α/β was measured in the lymph fluid (U/ml) using a bioassay. (C) Sheep ($n = 5$) were infected intravenously and subcutaneously with 1 and 5 ml blood, respectively, from a BTV8-infected viremic sheep. IFN-α/β in sera was measured using a bioassay. Significant differences between groups are indicated (*, $P < 0.05$; unpaired *t* test).

duced IFN-α/β production in lymph, peaking at day 6 with a-BTV2 (16 IU/ml) and at day 5 with BTV8 (12 IU/ml), which corresponds to the peak of viral dissemination by cDCs from skin (27) (Fig. 1A and B). IFN-α/β (Fig. 1A and B) and BTV (data not shown) were undetectable in lymph by day 10. We also found circulating IFN-α/β in the blood of sheep inoculated with BTV8 at days 2 and 6 postinjection (Fig. 1C). IFN-α/β reached basal levels in blood at day 10 postinjection. The viral load in blood peaked at day 6 (around 10^6 viral RNA copies/ml) and was decreased by 10-fold at day 10 (data not shown).

BTV induces IFN-α/β synthesis by LD lymph and blood cells independently of BTV strain and attenuation. Based on the data obtained as described above (Fig. 1), we hypothesized that lymph and blood pDCs and/or cDCs (the latter being early BTV targets [27]) could be activated by BTV to produce IFN-α/β. As a first approach, we simply enriched lymph and blood cells in cDCs and pDCs by low-density (LD) gradient centrifugation. We found that a rather low dose and wide range of BTV8 $TCID_{50}$ per cell [$(1 \text{ to } 50) \times 10^{-2}$] was efficient at triggering IFN-α/β synthesis in LD lymph and blood cells (Fig. 2A). The amount of IFN-α/β in the cell supernatant varied among animals (over 30 animals tested). Twenty-six BTV serotypes exist. We tested whether IFN-α/β induction would depend on viral strain and/or attenuation (vaccine strain). We used BTV strains that are representative of serotypes that have circulated in Europe since 2001, i.e., BTV1, -8, and -2. It was clear from our data that wild-type BTV2, BTV8, BTV1, and a-BTV2 each triggered IFN-α/β production by LD PBMCs, with no significant differences between strains (Fig. 2B).

pDCs are the main producers of IFN-α/β in lymph and blood cells. We proceeded to identify the cell type that was responsible for the IFN-α/β produced by the LD lymph and blood cells after BTV stimulation. In sheep lymph, cDCs are $CD11c^+$ cells and pDCs are characterized as B^- $CD11c^-$ $CD45RB^+$ cells, which can be isolated using immunomagnetic beads as previously described by us (52). No IFN-α/β could be detected in response to a-BTV2 in the lymph $CD11c^+$ cell fraction, while substantial amounts were found in the $CD11c^-$ cell fraction (500 IU/ml) (Fig. 3A). Lymph pDCs were isolated as described previously (52) and were found to produce IFN-α/β upon exposure to CpG-A (10,000 U/ml), poly(I·C)—a synthetic dsRNA analogue—in Lipofectamine 2000 (120 U/ml), and a-BTV2 (1,000 U/ml). Conversely, $CD11c^+$ and B^- $CD11c^-$ $CD45RB^-$ LD lymph cells were found to be unresponsive to CpG-A and Lipofectamine-transfected poly(I·C) (Fig. 3B and not shown). A specific anti-sheep IFN-α ELISA confirmed that BTV induced bona fide IFN-α in sheep lymph pDCs (Fig. 3C). In order to extend these results to blood cells, we purified $CD45RB^+$ and $CD45RB^-$ cells from LD PBMCs and confirmed that the IFN-α/β production in response to BTV was confined to the $CD45RB^+$ blood cell fraction (Fig. 3D). We then set up our goal to sort sheep blood pDCs to a high purity level using flow cytometry sorting. As shown in Fig. S1 in the supplemental material, upon CpG-A stimulation, IFN-α/β-producing cells were exclusively found among the $CD45RB^{high}$ B^- $CD11b^-$ $TCR\gamma/\delta^-$ $CD8^-$ $CD11c^-$ cells (see Fig. S1A to C). Furthermore, we separated the CD45R RB^{high} B^- $CD11b^-$ $TCR\gamma/\delta^-$

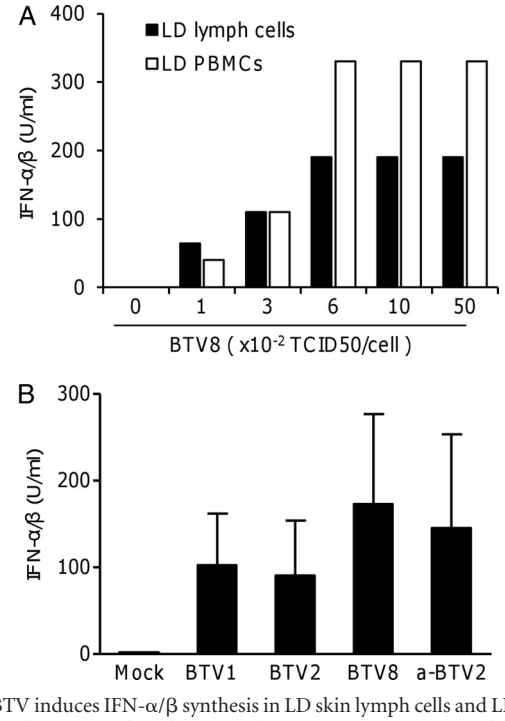

FIG 2 BTV induces IFN-α/β synthesis in LD skin lymph cells and LD PBMCs *in vitro* independent of viral strain and attenuation. (A) LD skin lymph cells and LD PBMCs from the same animal (1.5×10^6/ml) were cultured overnight with increasing doses of BTV8. The results of 1 representative experiment out of 5 are shown. (B) LD PBMCs from 5 sheep (1.5×10^6/ml) were cultured overnight with BTV strains BTV1, a-BTV2, BTV2, and BTV8 (0.06 $TCID_{50}$/cell). Culture supernatants were collected, and IFN-α/β was measured using a bioassay (U/ml). Means ± SEM are shown. There were no significant differences in IFN-α/β induction between strains ($P = 0.6$; Kruskal-Wallis test).

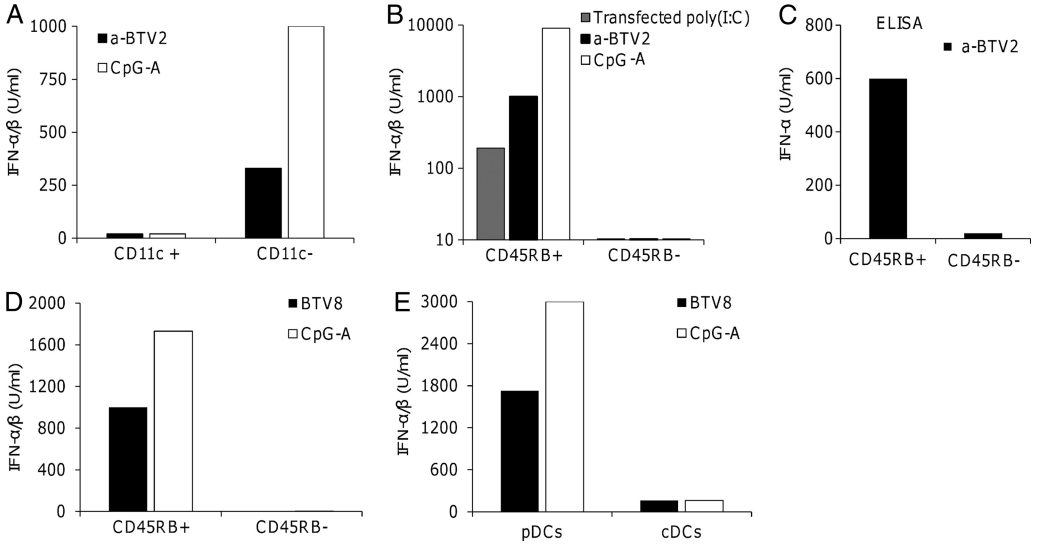

FIG 3 pDCs from lymph (A to C) and blood (D and E) are the main hematopoetic cell type producing IFN-α/β in response to BTV *in vitro*. (A) $CD11c^+$ and $CD11c^-$ cells were sorted from LD lymph cells with magnetic-activated cell sorting (MACS)-immunomagnetic beads and cultured (10^6/ml) overnight alone or with a-BTV2 (0.01 TCID per cell) or CpG-A (10 μg/ml). IFN-α/β was measured using a bioassay (U/ml). (B) MACS-sorted B^- $CD11c^-$ $CD45RB^+$ (pDCs) and control B^- $CD11c^-$ $CD45RB^-$ LD lymph cells were cultured overnight (10^5/ml) with lipofected poly(I·C) (200 ng plus 1 μl Lipofectamine 2000), a-BTV2 (0.01 $TCID_{50}$/cell), or CpG-A (10 μg/ml). IFN-α/β production was measured using a bioassay (U/ml). (C) MACS-selected B^- $CD11c^-$ $CD45RB^+$ and control B^- $CD11c^-$ $CD45RB^-$ LD lymph cells (10^5 cells/ml) were cultured overnight with a-BTV2 (0.01 $TCID_{50}$/cell), and IFN-α was measured in cultured supernatant using a ruminant-specific IFN-α ELISA. (D) MACS-sorted $CD45RB^+$ and $CD45RB^-$ cells from LD PBMCs (1.5×10^6 cells/ml) were cultured overnight with BTV8 (0.06 $TCID_{50}$/cell) or CpG-A (10 μg/ml). IFN-α/β was measured using a bioassay. (E) Blood pDCs (B^- $CD8^-$ $CD11b^-$ $CD11c^-$ $CD45RB^+$ FSC^{high}) and blood cDCs (B^- $CD8^-$ $CD11b^-$ $CD45RB^-$ $CD11c^+$ FSC^{high}) were sorted at 98% purity by flow cytometry (2.5×10^5 cells/ml) and stimulated overnight with BTV8 (0.06 $TCID_{50}$/cell) and CpG-A (10 μg/ml). IFN-α/β was determined in supernatants using a bioassay. Each experiment was repeated at least one or two times, and similar results were obtained. Note that due to the low numbers of purified pDCs that could be collected from 500 ml of blood in most instances, only single experimental pDC points could be done per animal. The results were confirmed by repeating the experiment with several animals.

$CD8^-$ $CD11c^-$ cells into small-, intermediate-, and large-sized cells (fractions 1, 2, and 3, respectively) based on the forward scatter (FSC) profile. As shown in Fig S1C, only fraction 1 (FSC^{high} cells) produced IFN-α/β in response to CpG. Fraction 1 also expressed high levels of the critical pDC transcriptional regulator TCF4 (9), much higher than cDCs did (see Fig. S1D). However, high TCF4 RNA levels were also found in fractions 2 and 3 (FSC^{low}) that do not produce IFN-α/β. These $TCF4^+$ $CD45RB^+$ FSC^{low} cells could correspond to mature pDCs that are smaller than immature pDCs and that do not respond to CpG-A in mice (5). We thus decided to sort "responsive" blood pDCs based on the $CD45RB^{high}$ B^-CD11b^- $TCR\gamma/\delta^-$ $CD8^-$ $CD11c^-$ FSC^{high} phenotype in the subsequent studies. Blood cDCs were sorted as being $CD11c^+$ B^- $CD11b^-$ $TCR\gamma/\delta^-$ $CD8^-$ $CD45RB^-$ FSC^{high} cells based on previously published phenotypic studies (3). From a sheep blood sample (400 ml), between 1 and 5×10^5 pDCs or cDCs could be sorted to high purity, which allowed us to undertake functional studies. When highly purified sheep blood primary pDCs and cDCs were sorted and stimulated with BTV8 or CpG-A, only pDCs produced IFN-α/β (Fig. 3E). As for lymph pDCs, we observed that the level of IFN-α/β produced by blood pDCs upon BTV stimulation was lower than that induced by CpG-A (Fig. 3A and E).

BTV infects pDCs but BTV replication is not mandatory for IFN-α/β synthesis in pDCs. IFN-α/β production by pDCs does not usually require viral replication but exceptions do exist (25, 30). Rotavirus was found to infect a small fraction of human blood primary pDCs, but IFN-α/β induction by rotavirus was found to be replication independent (11). We found that pDCs from BTV8-infected LD PBMC cultures (27%) were expressing the nonstructural NS2 protein, indicating that active viral infection occurs in sheep pDCs (Fig. 4A). Furthermore, when highly purified sheep blood pDCs were infected with BTV8, accumulation of viral RNA was detected after 48 h of culture (Fig. 4B). We then inactivated BTV8 using UV irradiation for different periods of time (see Fig. S2 in the supplemental material). After 20 min of UV irradiation of the viral inoculum (UV-BTV), viral replication could not be detected in LD lymph cells that included over 30% cDCs, the primary BTV target for viral replication, and around 2% pDCs (see Fig. S2A). However, IFN-α/β was still found to be produced in the supernatant of LD lymph cells (see Fig. S2B), although at a lower level than with live virus. IFN-α/β synthesis was further decreased with an increased duration of UV exposure, suggesting that UV treatment may possibly alter viral structures important for sensing in pDCs. Viral replication of UV-BTV8 (20 min of irradiation) could not be detected in BHK21 cells either (data not shown). UV-BTV preparations from 4 strains stimulated LD PBMCs to produce IFN-α/β, although at a significantly lower level than live BTV did (see Fig. S2C). Heat-inactivated preparations were inefficient (see Fig. S2C). We confirmed that UV-BTV did not replicate in pDCs from BTV-infected LD PBMC cultures (Fig. 4A) or in the purified pDCs (Fig. 4B). There again, UV-BTV8 still induced IFN-α/β in highly purified blood pDCs, although to a lower extent than live BTV8 (Fig. 4C).

BTV is a very difficult virus to purify, and therefore, crude BTV-infected BHK21 cell supernatants were used to stimulate pDCs in the above-described experiments. We nevertheless successfully purified BTV1 by sucrose gradient centrifugation (46)

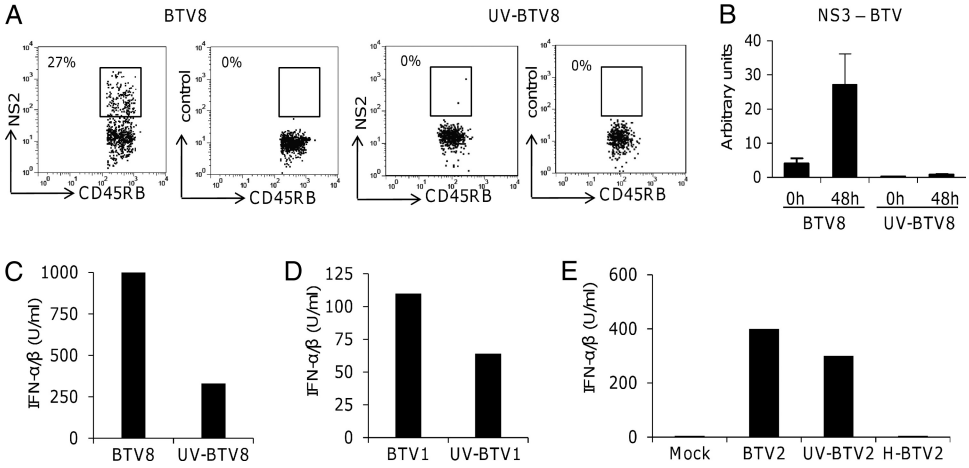

FIG 4 BTV replicates in pDCs but replication is dispensable for IFN-α/β induction. (A) LD PBMCs were infected with BTV8 or UV-BTV8 (0.06 $TCID_{50}$/cell) or were left untreated and were incubated for 48 h at 37°C. The B^+ $CD8^+$ $TCR\gamma/\delta^+$ $CD11b^+$ $CD11c^+$ cells were gate excluded, and the $CD45RB^+$ FSC^{high} cells were analyzed for NS2 expression (% shown). NS2-specific expression was controlled with nonimmune rabbit serum (control). The experiment was reproduced 3 times with similar results. (B) FACS-sorted blood pDCs (2.5×10^5/ml) were cultured with BTV8 or UV-BTV8 (0.06 $TCID_{50}$/cell). Total RNA was extracted 48 h after infection. Expression of NS3-BTV RNA relative to that of GAPDH was determined by qRT-PCR, and arbitrary units were calculated using the $2^{-\Delta CT}$ method (mean results ± SEM from 2 independent cultures). (C) FACS-sorted pDCs (2.5×10^5 cell/ml) were cultured alone or with BTV8 or UV-BTV8 (0.06 TCID/cell). IFN-α/β was detected using a bioassay (U/ml). (D) FACS-sorted pDCs (2.5×10^5 cells/ml) were cultured overnight with sucrose gradient-purified BTV1 and UV-BTV1 (3 μg/ml, around 0.01 TCID/cell). The supernatants were collected, and type I IFN was measured using a bioassay (U/ml). (E) pDCs were selected from LD lymph cells using MACS beads. They were cultured overnight (1.5×10^6 cells/ml) alone (mock) or with a-BTV2 (0.01 $TCID_{50}$/cell), UV-inactivated a-BTV2 (0.01 $TCID_{50}$/cell), or heat-inactivated a-BTV2 (H-BTV2) (0.01 $TCID_{50}$/cell). IFN-α/β was detected (U/ml) in the culture supernatant using a bioassay.

and found that purified BTV1 and UV-BTV1 both induced IFN-α/β in highly purified sheep blood pDCs (Fig. 4D), indicating that cell culture contaminants were not responsible for IFN-α/β induction in pDCs. Lymph pDCs were also induced to produce IFN-α/β upon UV-a-BTV2 stimulation. However, as found with LD PBMCs (see Fig. S2C in the supplemental material), heat-inactivated BTV (Fig. 4E) and binary ethyleneimine-inactivated BTV from a commercial vaccine (without adjuvant; data not shown) were not capable of IFN-α/β induction in pDCs, suggesting that specific structural viral motifs need to be preserved to ensure proper sensing for IFN-α/β induction in pDCs.

BTV induces the expression of several cytokine genes in addition to IFN-α, as well as surface CD80/86, in primary sheep blood pDCs. Since pDCs have been shown to produce other cytokines besides IFN-α/β in mice and humans, we determined whether other cytokines, which are likely to have a strong impact on the immune response triggered by the virus, were induced by BTV in sheep pDCs. Indeed, live purified BTV1, UV-BTV1, and crude UV-BTV8 were all found to induce IFN-α, TNF-α, IL-6, and IL-12 gene expression in purified sheep blood pDCs (Fig. 5B and C). UV-BTV8 was also found to increase the expression of the costimulatory CD80/86 molecules on the cell surface of the pDCs from LD PBMC cultures (Fig. 5A, median fluorescence intensity of 66 for unstimulated and 172 for BTV-activated pDCs).

IFN-α/β induction by UV-BTV in purified pDCs involves endo-/lysosomal maturation. So far, our data have shown that BTV triggers IFN-α/β secretion, as well as the expression of other cytokine genes and costimulatory molecules, in primary sheep pDCs by a mechanism that does not require viral replication. In order to investigate the mechanism of IFN-α/β induction in pDCs, we used UV-BTV stimulation to avoid possible interference between IFN-α/β synthesis and viral replication. We first addressed whether IFN-α/β induction by UV-BTV required intracellular processing via endo-/lysosomal vesicle maturation. We used bafilomycin A1, an ATPase-specific inhibitor that blocks endosomal and lysosomal acidification. We found that bafilomycin A1 abrogated the IFN-α/β production by LD PBMCs and purified pDCs that were stimulated with either UV-BTV8 or CpG-A (Fig. 6A and B). Chloroquine, which is largely used as an inhibitor of endo-/lysosomal maturation, also prevented the IFN-α/β synthesis induced by UV-BTV in LD PBMCs and in highly purified blood pDCs. However, chloroquine did not affect the IFN-α/β synthesis induced by poly(I·C) delivered with Lipofectamine 2000, which accesses the cytosol without need for endosomal routing (69) (Fig. 6C and D). Cell viability was found to be unaltered by these drug treatments (see Fig. S3A and B in the supplemental material).

IFN-α/β induction by UV-BTV involves TLR7-independent and MyD88-dependent signaling. The inhibition of IFN-α/β induction by inhibitors of endolysosomal maturation suggests that a TLR-mediated signaling may be involved in the IFN-α/β induction by UV-BTV, as is usually the case with pDCs stimulated by viruses. TLR7 is known to mainly sense single-stranded viral RNAs, but it was shown to also respond to specific tertiary dsRNA structures (29). We therefore tested the effect of A151, an oligonucleotide described as a TLR antagonist that inhibits TLR7 and, to a lesser extent, TLR9. A151 at a 50-μg/ml concentration potently inhibited the synthesis of IFN-α/β induced in sheep LD PBMCs by inactivated influenzavirus and, to a lesser extent, by CpG-A, as expected. However, even at a 50-μg/ml concentration, A151 did not inhibit the IFN-α/β induction by UV-BTV (Fig. 7). As A151 strongly inhibited influenza virus-induced IFN-α/β that can signal through TLR7 and -8, this implies that UV-BTV acti-

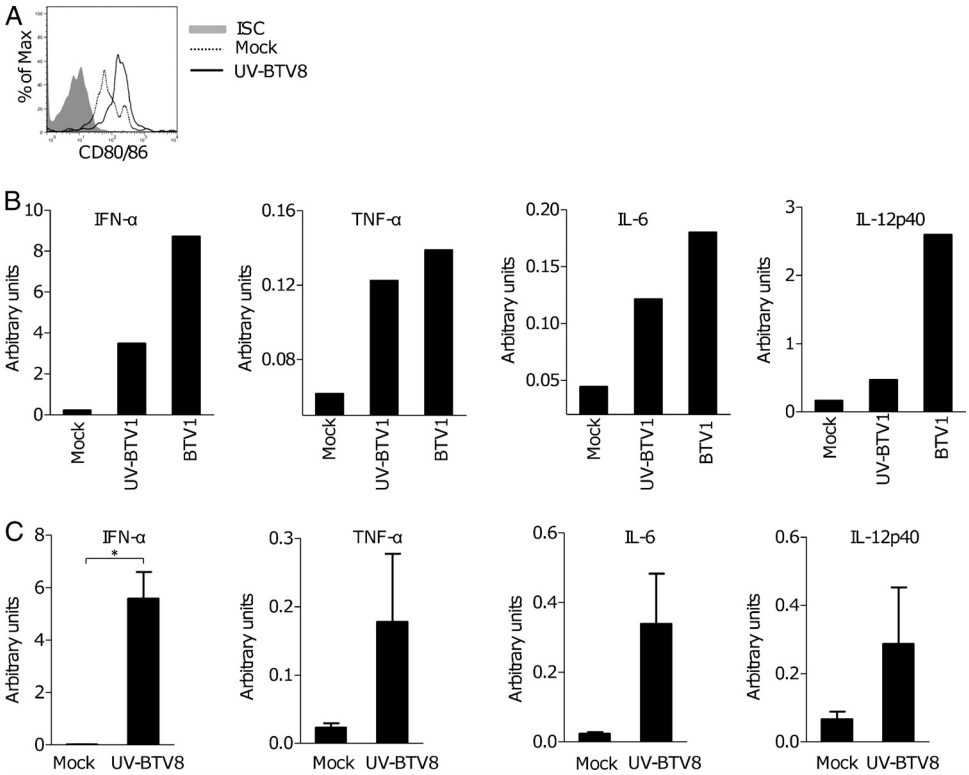

FIG 5 UV-BTV increases CD80/86 surface expression and activates cytokine gene expression in blood pDCs. LD PBMCs were cultured alone (mock) or with UV-BTV8 (0.06 $TCID_{50}$/ml). Cells were stained for pDC markers (see Fig. 4A legend) and for CD80/86 surface detection. (A) FACS histogram of CD80/86 and isotype control (ISC) expression on gated pDCs is presented. (B) FACS-sorted pDCs from one sheep (2.5×10^5 cells/ml) were cultured overnight alone or with BTV1 (sucrose gradient purified, 3 μg/ml) or UV-BTV1 (sucrose gradient purified, 3 μg/ml). Cytokine gene expression relative to that of GAPDH was assessed by qRT-PCR, and arbitrary units were calculated by the $2^{-\Delta CT}$ method. (C) FACS-sorted pDC preparations from 3 different sheep were stimulated overnight by UV-BTV8 (0.06 $TCID_{50}$/cell), and cytokine gene expression was evaluated as described for panel B (means ± SEM are shown). *, $P < 0.05$; paired *t* test.

vates IFN-α/β production via a TLR7/8-independent mechanism. Note that bovine pDCs do not express TLR8 mRNA (20).

Although TLR7 did not appear to play any role in the IFN-α/β induction by UV-BTV, we asked whether the MyD88 adaptor molecule could be involved in that process. Indeed, MyD88 not only mediates TLR7 and TLR9 signaling but is also involved in TLR-independent pathways of IFN-α/β induction, such as in the case of the DNA virus sensor DHX36 box helicase in pDCs (36). As RNA interference cannot be used in primary pDCs, in which these molecules induce IFN-α/β by themselves (29), we used a *MyD88* homodimerization inhibitor peptide that binds to the MyD88 TIR domain and that is fused to an antennapedia-derived cell permeant motif (43). LD PBMCs from 5 different sheep were cultured overnight with the MyD88 inhibitory peptide or the control peptide and then activated with CpG-A or with UV-BTV for 12 h. Whereas the control peptide, i.e., the antennapedia cell permeant motif, marginally affected the IFN-α/β secretion induced by CpG-A (87% ± 7% [mean ± SEM] of the level in the control) and UV-BTV (83% ± 10% of the level in the control), the MyD88 inhibitory peptide at the 100 μM dose significantly reduced the IFN-α/β production induced both by CpG (28% ± 8% of the level in the control) and BTV (40% ± 6% of the level in the control) (Fig. 8). We could not use the MyD88 inhibitory peptide and its control on purified pDCs for subsequent stimulation by UV-BTV because the sorting procedure compromised the viability of the cells and, thus, the cells did not survive the subsequent preincubation with both the control and the inhibitory peptides. However, the viability of fresh LD PBMCs was not significantly affected by the peptides (see Fig. S3C in the supplemental material). As the only cells capable of IFN-α/β production in LD PBMCs are pDCs (Fig. 3), we can conclude that UV-BTV signaling for IFN-α/β synthesis in pDCs involves, at least in part, the MyD88 adaptor, independent of TLR7/8 activation.

IFN-α/β induction by UV-BTV in pDCs implicates PKR- and JNK-dependent signaling pathways. The cytosolic serine-threonine kinase PKR has been implicated in the IFN-α/β production induced by viruses in many cell types, including cDCs (13, 56), but is not yet studied in pDCs. PKR activation can occur by direct binding of dsRNA or can be induced downstream of other nucleic acid sensors, such as TLR (30) or, possibly, MDA-5 (56, 60). In order to assess the contribution of PKR in the IFN-α/β production induced by UV-BTV, we treated LD PBMC cultures, as well as purified blood pDCs, with 2-aminopurine (2-AP), a commonly used PKR inhibitor (66), or with the oxindole-imidazole C16, a reported selective PKR inhibitor that is efficient in different cell types from different species (2, 21, 24, 31, 33). Because anti-sheep PKR and P-PKR antibodies are not available, we confirmed that C16 used at a 500 nM concentration was potent at preventing PKR phosphorylation induced by poly(I·C) in HeLa cells (data not shown). Both drugs potently inhibited IFN-α/β secretion in LD PBMCs (Fig. 9A and B) while maintaining cell viability (see Fig. S3D and E in the supplemental material). Both

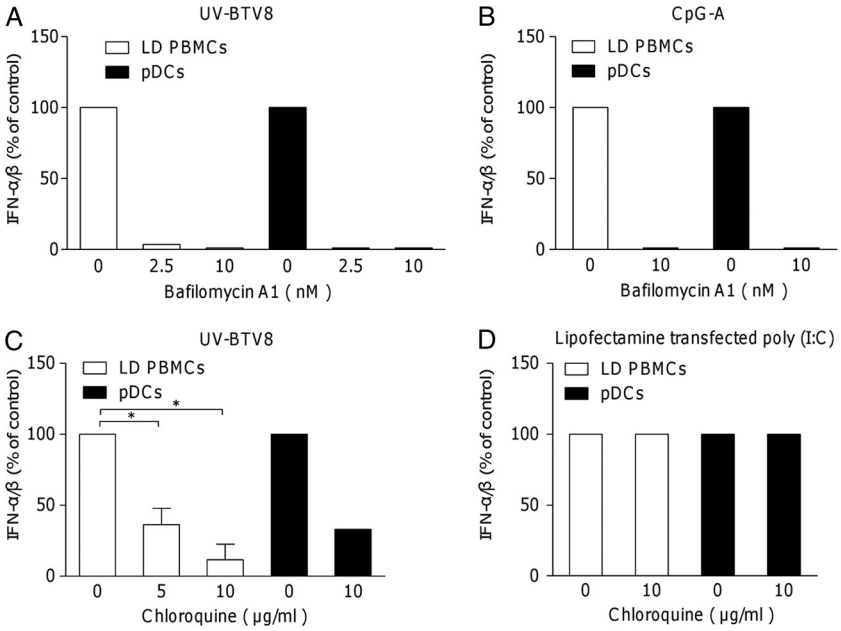

FIG 6 UV-BTV8-induced type I IFN in blood pDCs is sensitive to bafilomycin A1 (A, B) and chloroquine (C, D). (A and B) LD PBMCs (1.5×10^6 cells/ml) (left) and FACS-sorted pDCs (2.5×10^5 cells/ml) (right) were treated with bafilomycin A1 (2.5 and 10 μg/ml) for 30 min prior to UV-BTV8 (0.06 $TCID_{50}$/ml) (A) and CpG-A (10 μg/ml) (B) exposure. After overnight culture, IFN-α/β was measured (U/ml) in supernatants by bioassay. Data are expressed as the percentage of the IFN-α/β level obtained without drug. (C and D) LD PBMCs (3×10^5 cells/well) (left) and FACS-sorted pDCs (5×10^4 cells/well) (right) were treated with chloroquine (5 and 10 μg/ml) for 30 min prior to UV-BTV8 (0.06 $TCID_{50}$/ml) (C) and poly(I·C) (200 ng plus 1 μl Lipofectamine 2000) exposure (D). After overnight stimulation, supernatants were collected and IFN-α/β was measured using a bioassay (U/ml). Data are expressed as the percentage of the IFN-α/β level obtained without drug. Single experimental points from one sheep were used in panels A, B, and D and the filled (pDC) bars of panel C, and single experimental points from three sheep LD PBMCs (means ± SEM) were used the empty bars in panel C. *, $P < 0.05$; paired *t* test.

drugs also strongly reduced the IFN-a, TNF-a, and IL-12 mRNA expression induced by UV-BTV in purified pDCs (Fig. 9D), whereas they did not affect the CD80/CD86 expression level induced by UV-BTV at the cell surface of pDCs (Fig. 9C).

As PKR was shown to modulate IFN-α/β mRNA poly(A) integrity in rotavirus-infected mouse embryonic fibroblasts and in cDCs infected with some specific RNA viruses, we tested whether the oxindole-imidazole C16 treatment would decrease the proportion of polyadenylated versus total IFN-α mRNA induced by UV-BTV. As shown in Fig. S4 in the supplemental material, C16 decreased the IFN-α/β mRNA amounts detected by random hexamer (total RNA)- and oligo(dT) (polyadenylated RNA)-primed reverse transcription to a similar extent. Thus, blockade of PKR enzymatic activity by C16 does not specifically affect the amounts of polyadenylated IFN-α/β mRNA in UV-BTV-treated pDCs, suggesting that the PKR-mediated increase of IFN-α/β mRNA does not involve regulation of IFN-α/β mRNA polyadenylation.

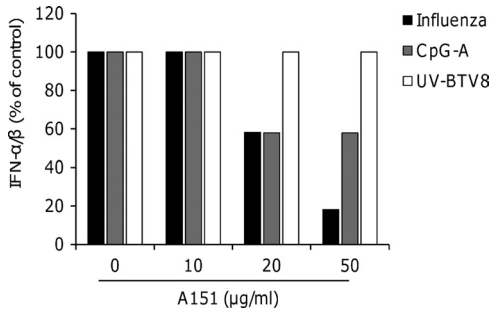

FIG 7 The TLR7/9 inhibitor A151 does not affect IFN-α/β induction by UV-BTV in LD PBMCs. Freshly isolated LD PBMCs were preincubated with increasing doses of the TLR7/9 inhibitor A151 for 30 min and further stimulated overnight with UV-BTV8 (0.06 TCID/cell), CpG (10 μg/ml), or formol-inactivated influenzavirus (4 μg/ml). IFN-α/β was detected in supernatants by a bioassay. The IFN-α/β amounts induced by influenza virus, CpG-A, and UBTV8 were 110, 190, and 64 IU/ml, respectively. The experiment was reproduced twice and gave the same results.

PKR is known to activate mitogen-activated protein kinases (MAPK), such as stress-activated protein kinase (SAPK)/JNK (22), which has also been implicated in the induction of IFN-α/β production by cDCs upon adenovirus stimulation (15). LD PBMCs and purified pDCs were cultured with UV-BTV in the presence of SP600125 (a SAPK/JNK inhibitor) (4, 12, 32, 45) and PD184325 (an inhibitor of ERK1/2, which is another member of the MAPK family) (64). We found that UV-BTV IFN-α/β induction was inhibited by the SAPK/JNK inhibitor by over 60% (Fig. 10B), whereas the ERK1/2 inhibitor had no effect (Fig. 10A). No toxicity was found for the SAPK/JNK inhibitor (see Fig. S3F in the supplemental material).

Altogether, our data show that the induction of IFN-α/β by UV-BTV in pDCs involves a TLR7/8-independent and MyD88-dependent mechanism. Based on the use of pharmacological inhibitors, they also implicate PKR- and SAPK/JNK-dependent mechanisms.

DISCUSSION

Our study reveals novel information concerning the interactions between the dsRNA virus BTV and primary dendritic cell subsets for the induction of IFN-α/β, a key innate immunity cytokine that

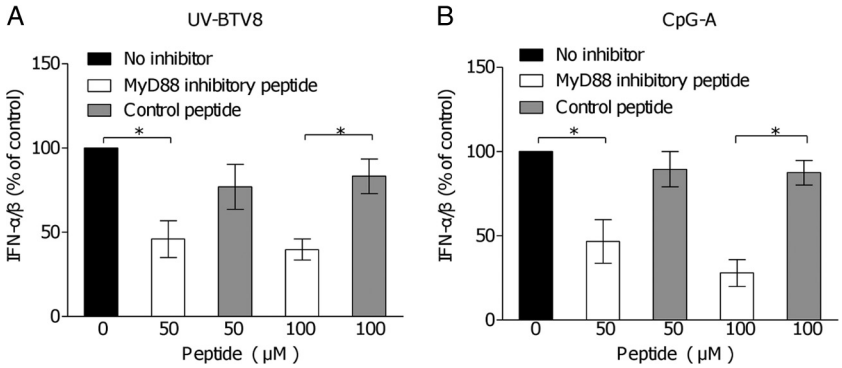

FIG 8 Inhibition of MyD88 homodimerization reduces IFN-α/β release by sheep LD PBMCs in response to UV-BTV8 and CpG-A. LD PBMCs from 4 sheep (3×10^5 cells/well) were incubated overnight alone or with MyD88 inhibitory peptide or control peptide and then were stimulated for 12 h with UV-BTV8 (0.06 $TCID_{50}$/ml) (A) and CpG-A (10 μg/ml) (B). IFN-α/β was measured (U/ml) in the supernatants using a bioassay. The IFN-α/β amounts induced by UV-BTV were 16, 31, 63, and 500 IU/ml for the 4 different sheep, respectively. The IFN-α/β amounts induced by CpG-A were 62.5, 125, 250, and 1,000 IU/ml. Data are expressed as the percentages of the IFN-α/β level obtained without peptide treatment. Means ± SEM are shown. *, $P < 0.05$; paired *t* test.

is instrumental for optimal CD8 T cell and antibody responses (39, 41, 51) and for direct antiviral defense. We showed that BTV displays specific interactions with primary pDCs and cDCs: while it infects both cell types, it induces IFN-α/β only in pDCs without requiring viral replication, via a mechanism involving endocytosis and signaling through the MyD88 adaptor without TLR7/8 engagement. Our data show for the first time the involvement of MyD88 in dsRNA virus signaling in pDCs. Thus, MyD88 remains the only known transducing molecule in pDCs for type I IFN induction. However, the evidences presented here from our BTV study demonstrate clearly that viral sensors other than TLR7/8 can be used in pDCs, as was found for TLR9 with some DNA viruses that can alternatively use the DHX36 helicase in pDCs (36).

Although IFN-α/β was detected in blood and lymph early after *in vivo* BTV infection, it was no longer detected in lymph and blood by day 10. BTV has disappeared in lymph at that time, but relatively high viral loads were still detectable in blood, as previously reported by several authors (49, 53). The lack of IFN-α/β detection in blood at day 10 could be related to the decreased number of pDCs in blood that has been observed in the course of

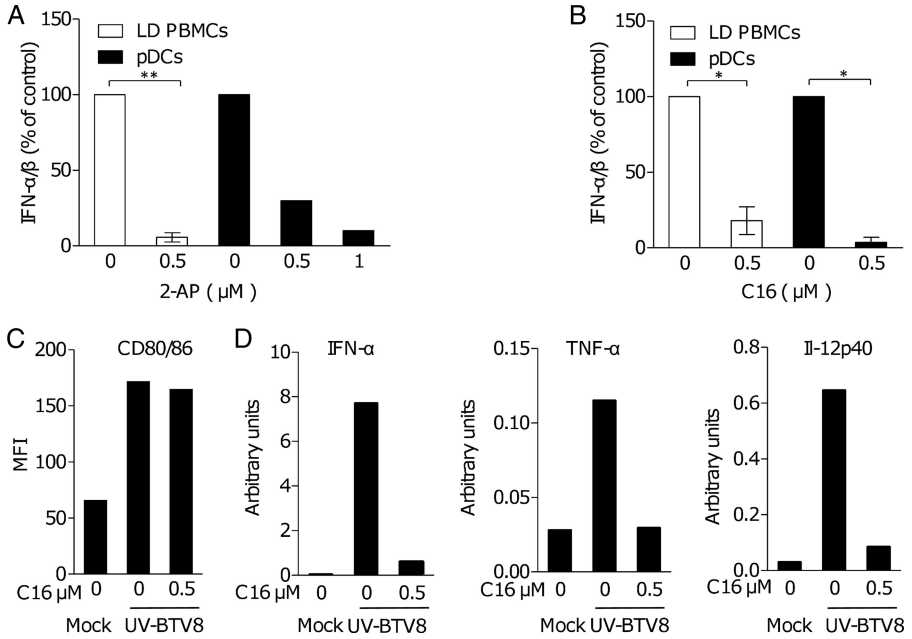

FIG 9 PKR inhibition reduces IFN-α/β release and cytokine gene activation by blood pDCs in response to UV-BTV8. (A, B) 2-AP (A) and C16 (B) were used to block PKR activation in LD PBMCs (empty bars) and FACS-sorted pDCs (filled bars). Drugs were added to cells at indicated concentrations for 30 min before infection, and cells were stimulated overnight with UV-BTV8. IFN-α/β was measured (U/ml) in supernatants using a bioassay. Data are expressed as the percentages of the IFN-α/β level obtained without drug treatment. Data expressed as means ± SEM were obtained with 3 different sheep. *, $P < 0.05$; paired *t* test. (C) LD PBMCs were treated or not with C16 (0.5 μM) and were exposed to UV-BTV8 (0.06 $TCID_{50}$/ml) for 48 h. Cells were stained for pDC and CD80/86 detection by FACS analysis. The histogram represents the medians of fluorescence intensity (MFI) of CD80/86 expression on pDCs. (D) FACS-sorted pDCs were incubated with C16 (0.5 μM) for 30 min prior to UV-BTV8 stimulation and cultured overnight. Cytokine gene expression (IFN-α, TNF, and IL-12p40) was determined by qRT-PCR.

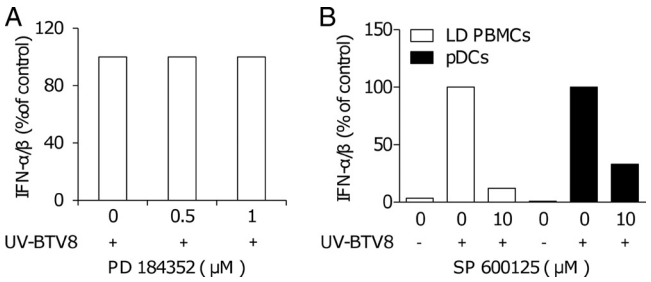

FIG 10 SAPK/JNK but not MEK1/ERK1/2 inhibition reduces IFN-α/β production in response to UV-BTV8. (A) LD PBMCs (1.5×10^6 cells/ml) were treated with indicated doses of PD184352 (MEK1/ERK1/2 inhibitor) for 30 min before overnight culture with UV-BTV8 (0.06 $TCID_{50}$/ml). (B) LD PBMCs (1.5×10^6 cells/ml) and pDCs (2.5×10^4 cells/ml) were incubated with the SAPK/JNK inhibitor SP600125 (10 μM) for 30 min before stimulation with UV-BTV8 (0.06 $TCID_{50}$/ml). IFN-α/β was measured (U/ml) in culture supernatants by bioassay. Data are expressed as the percentages of the IFN-α/β level obtained without drug treatment. The results of 1 representative experiment of 2 are shown.

many viral infections, due to selective apoptosis (65). Among other hypotheses, it is also possible that the association of BTV with erythrocytes during viral clearance at day 10 prevents effective interactions between BTV and pDCs (44).

The specific induction of IFN-α/β in pDCs and not in cDCs, even with live virus, could be explained by cell type-specific molecular mechanisms, such as the expression of proper sensors, subcellular trafficking, and transducing cascades. Regarding cell type-specific sensors for IFN-α/β induction by viruses, sensing of Newcastle disease virus in cDCs largely relies on RIG-I helicase, whereas it relies on TLR7 in pDCs (35). The lack of IFN-α/β synthesis by cDCs that permit replication of BTV may also involve the expression of nonstructural proteins that block IFN-α/β synthesis. Indeed, BTV NS1 and NS2 appear to interfere with the interferon regulatory factor (IRF-3 and -7) response in HeLa cells (62). Following that scenario, the pDC fraction that expresses BTV may not be producing IFN-α/β, as shown for rotavirus in pDCs (11). However, we could not test whether viral expression and IFN-α/β were exclusive phenomena in BTV-infected pDCs cultures as no anti-sheep IFN-α/β antibody exists to label intracellular IFN-α/β.

Our mechanistic investigations show that endo-/lysosomal acidification and maturation are required for IFN-α/β induction by UV-BTV in pDCs, similar to what is found with rotavirus IFN-α/β induction in human pDCs (11). This finding indicates that an intracellular vesicular processing of BTV is required for appropriate sensing and signaling. Notably, early endosomal low pH was also shown to be essential for BTV uncoating in mammalian cells (17). The UV-BTV elements that are sensed for triggering IFN-α/β synthesis within pDCs could be dsRNA structures from the core and/or proteins of the capsid. In order to test the role of protein capsid components, we stimulated sheep pDCs with sucrose gradient-purified virus-like particles produced from recombinant baculoviruses (not shown); however, the control mock fractions of the empty baculovirus-infected insect cell cultures also induced large amounts of IFN-α/β, probably due to the presence of baculovirus remnants (28). However, the protein structures may more likely be involved in the entry mechanism of the virus and in the proper addressing to subcellular compartments rather than in the sensing by pathogen recognition receptors. Indeed only enveloped viruses were found capable of activating pDCs for IFN-α/β production via non-nucleic acid structures, although this pathway is thought to be marginal compared to the nucleic acid one (7, 16). Furthermore, in the case of rotavirus in human pDCs, the rotaviral dsRNA encapsidated in intact virus particles was found to be the likely signal for IFN activation (11). However, the integrity of the capsid proteins and/or of the dsRNA structures appeared to be very important for leading to optimal IFN-α/β production, as prolonged UV irradiation of BTV reduced the level of IFN production in sheep lymph cells (see Fig. S2 in the supplemental material).

The requirement for endo-/lysosomal acidification may also indicate that BTV was sensed in pDCs via a TLR-dependent mechanism. Both TLR3 (1) and TLR7 (29) can sense dsRNA. However, TLR3 mainly plays a role in epithelial cells for IFN-α/β induction (69) and it is not expressed by pDCs in mice and humans (42, 55). In sheep pDCs, poly(I·C) does not induce type I IFN unless it is introduced into the cytosol by lipofection (data not shown), thus excluding TLR3 as an endosomal dsRNA sensor. In addition, we demonstrated that the A151 TLR7/9 inhibitor was not efficient at blocking UV-BTV-induced IFN-α/β, whereas it was efficient at blocking the IFN-α/β production induced by influenza virus. This finding excludes the possibility of both TLR7 and TLR8 involvement in UV-BTV signaling in pDCs.

The lack of TLR7 involvement in IFN-α/β induction in pDCs by an RNA virus as described here is a very rare event. Independence of TLR7 has also been reported for the respiratory syncytial paramyxovirus, which enters and signals via an unknown mechanism in human pDCs after plasma membrane fusion, and not via an endosomal pathway (30). The other known viral sensors in pDCs are DNA sensors, i.e., TLR9 and the DHX36 helicase, which both signal via MyD88. TLR9 is endosomal, while DHX36 is cytosolic. It could be possible that UV-BTV dsRNA reaches the pDC cytosol after uncoating and triggers (a) cytosolic helicase(s) that remain(s) to be identified. The known RIG-1/MDA-5/LGP2/DDX1 helicases (40, 67, 68, 69) can all bind various forms of dsRNA, and they all signal via the mitochondrial adaptor MAVS (also named IPS-1/Cardif/VISA) (59). However, mouse pDCs appear not to rely on MAVS for IFN-α/β induction by viruses (63). Thus, our results suggest the hypothesis that dsRNA sensors, possibly novel helicases linked to MyD88, are implicated in *Reoviridae*-induced IFN-α/β in pDCs.

PKR is the first dsRNA cell sensor that has been described. Its autophosphorylation and dimerization upon dsRNA binding primarily lead to the establishment of an antiviral state, but it can also trigger IFN-α/β synthesis in different cell types, including cDCs (13), via multiple, complex, and sometimes controversial mechanisms. In human pDCs, the PKR inhibitor 2-AP was found to prevent the IFN-α/β secretion induced by CpG-A (30), indicating that PKR can integrate signal transduction from TLR in this cell type. Some published reports indicate that PKR can control the expression and activation of IRF3 and IRF1, as well as the activation of NF-κB (18, 37, 38, 50), thus having an impact on IFN-α/β gene transcription. In the case of rotavirus-infected embryonic fibroblasts, PKR was shown to promote IFN-α/β secretion not by an increase of transcriptional activity but at the posttranscriptional level via a yet-to-be-defined mechanism (60). Significantly, PKR was recently found to induce IFN-α/β production in coordination with MDA-5 activation by some viruses via the stabilization of IFN-α/β mRNA poly(A) (56). Thus, PKR can promote

IFN-α/β production by many mechanisms, although it has not been studied in pDCs. In the case of BTV in pDCs, PKR activation could be direct, via intracytosolic sensing of dsRNA, or indirect, as for TLR signaling. Our results indicate that UV-BTV increases IFN-α/β synthesis and IFN-α mRNA production by a mechanism independent of stabilization of mRNA polyadenylation. Finally, possibly downstream or independently of PKR, we found that signaling via JNK was implicated in IFN-α/β production induced by UV-BTV in primary pDCs, whereas ERK1/2 signaling was not involved. Adenovirus that triggered IFN-α/β production via TLR and MAVS-independent mechanisms in cDCs also used JNK-dependent and ERK1/2-independent signaling related to sensors that were not identified (15).

Altogether, our data show that a dsRNA virus triggers IFN-α/β in primary host pDCs via a novel mechanism that is independent of TLR7/8 but dependent on the MyD88 adaptor. We bring some indications that the PKR and JNK signaling pathways may also be involved. Other members of the *Reoviridae* family, such as members of the genera *Rotavirus* and *Orbivirus*, may use similar pathways, associated with a restriction of IFN-α/β production in pDCs (47). Our findings aid in the understanding of BTV pathogenicity and, importantly, will have impacts on the improvement of vaccine development against dsRNA viruses. For example, in order to induce optimal adaptive immune responses, industrial processes of viral inactivation must maintain the ability of BTV and/or other reovirus particles to trigger IFN-α/β production by pDCs.

ACKNOWLEDGMENTS

We thank the Unité Commune d'Expérimentation in Jouy-en-Josas (France) for their care of the cannulated sheep and for providing sheep blood pouches, the Centre d'Imagerie Interventionnelle for their support in sheep cannulation, the Centre de Recherche Biomédicale in Maisons-Alfort (France) for the BTV infection of cannulated sheep, and the Plate Forme d'Infectiologie Expérimentale INRA (Nouzilly, France) for performing BTV8 infections and serum collections. We are grateful for the help of Frédérick Arnaud (Lyon, France). We thank François Lefèvre for JNK and MEK inhibitors. We thank Jacques Hugon and François Mouton-Liger (Hopital Lariboisière, Paris, France) for their support and help in the PKR assays. We thank Olivier Schwartz for providing the A151 TLR7/9 inhibitor and Nicolas Bertho for the gift of influenzavirus. We thank Antonio Cosma and Sabrina Guenounou (Plate-forme d'Immunomonitoring, Centre d'Energie Atomique, Fontenay aux Roses, France) for the first precious pDC sorting. We thank Sanofi-Aventis for the gift of Lovenox.

This work was supported by the Agence Nationale pour la Recherche (VacGenDC ANR 06 GANI 015-03) and by the EMIDA Era-Net (OrbiNet 2009).

REFERENCES

1. **Alexopoulou L, Holt AC, Medzhitov R, Flavell RA.** 2001. Recognition of double-stranded RNA and activation of NF-kappaB by Toll-like receptor 3. Nature **413**:732–738.
2. **Arnaud N, et al.** 2010. Hepatitis C virus controls interferon production through PKR activation. PLoS One **5**:e10575.
3. **Bastos RG, Johnson WC, Brown WC, Goff WL.** 2007. Differential response of splenic monocytes and DC from cattle to microbial stimulation with Mycobacterium bovis BCG and Babesia bovis merozoites. Vet. Immunol. Immunopathol. **115**:334–345.
4. **Bennett BL, et al.** 2001. SP600125, an anthrapyrazolone inhibitor of Jun N-terminal kinase. Proc. Natl. Acad. Sci. U. S. A. **98**:13681–13686.
5. **Bjorck P, Leong HX, Engleman EG.** 2011. Plasmacytoid dendritic cell dichotomy: identification of IFN-{alpha} producing cells as a phenotypically and functionally distinct subset. J. Immunol. **186**:1477–1485.
6. **Broquet AH, Hirata Y, McAllister CS, Kagnoff MF.** 2011. RIG-I/MDA5/MAVS are required to signal a protective IFN response in rotavirus-infected intestinal epithelium. J. Immunol. **186**:1618–1626.
7. **Charley B, Lavenant L, Delmas B.** 1991. Glycosylation is required for coronavirus TGEV to induce an efficient production of IFN alpha by blood mononuclear cells. Scand. J. Immunol. **33**:435–440.
8. **Chevallier N, et al.** 1998. Bovine leukemia virus-induced lymphocytosis and increased cell survival mainly involve the CD11b+ B-lymphocyte subset in sheep. J. Virol. **72**:4413–4420.
9. **Cisse B, et al.** 2008. Transcription factor E2-2 is an essential and specific regulator of plasmacytoid dendritic cell development. Cell **135**:37–48.
10. **Contreras V, et al.** 2010. Existence of CD8{alpha}-like dendritic cells with a conserved functional specialization and a common molecular signature in distant mammalian species. J. Immunol. **185**:3313–3325.
11. **Deal EM, Jaimes MC, Crawford SE, Estes MK, Greenberg HB.** 2010. Rotavirus structural proteins and dsRNA are required for the human primary plasmacytoid dendritic cell IFNalpha response. PLoS Pathog. **6**:e1000931.
12. **Deng L, et al.** 2011. Hepatitis C virus infection promotes hepatic gluconeogenesis through an NS5A-mediated, FoxO1-dependent pathway. J. Virol. **85**:8556–8568.
13. **Diebold SS, et al.** 2003. Viral infection switches non-plasmacytoid dendritic cells into high interferon producers. Nature **424**:324–328.
14. **Edwards AD, et al.** 2003. Toll-like receptor expression in murine DC subsets: lack of TLR7 expression by CD8 alpha+ DC correlates with unresponsiveness to imidazoquinolines. Eur. J. Immunol. **33**:827–833.
15. **Fejer G, et al.** 2008. Key role of splenic myeloid DCs in the IFN-alphabeta response to adenoviruses in vivo. PLoS Pathog. **4**:e1000208.
16. **Fitzgerald-Bocarsly P, Dai J, Singh S.** 2008. Plasmacytoid dendritic cells and type I IFN: 50 years of convergent history. Cytokine Growth Factor Rev. **19**:3–19.
17. **Forzan M, Marsh M, Roy P.** 2007. Bluetongue virus entry into cells. J. Virol. **81**:4819–4827.
18. **Garcia MA, et al.** 2006. Impact of protein kinase PKR in cell biology: from antiviral to antiproliferative action. Microbiol. Mol. Biol. Rev. **70**:1032–1060.
19. **Garcia MA, Meurs EF, Esteban M.** 2007. The dsRNA protein kinase PKR: virus and cell control. Biochimie **89**:799–811.
20. **Gibson A, Miah S, Griebel P, Brownlie J, Werling D.** 2012. Identification of a lineage negative cell population in bovine peripheral blood with the ability to mount a strong type I interferon response. Dev. Comp. Immunol. **36**:332–341.
21. **Gilfoy FD, Mason PW.** 2007. West Nile virus-induced interferon production is mediated by the double-stranded RNA-dependent protein kinase PKR. J. Virol. **81**:11148–11158.
22. **Goh KC, deVeer MJ, Williams BR.** 2000. The protein kinase PKR is required for p38 MAPK activation and the innate immune response to bacterial endotoxin. EMBO J. **19**:4292–4297.
23. **Gohin I.** 1997. The lymphatic system and its functioning in sheep. Vet. Res. **28**:417–438.
24. **Gray JS, Bae HK, Li JC, Lau AS, Pestka JJ.** 2008. Double-stranded RNA-activated protein kinase mediates induction of interleukin-8 expression by deoxynivalenol, Shiga toxin 1, and ricin in monocytes. Toxicol. Sci. **105**:322–330.
25. **Guzylack-Piriou L, Bergamin F, Gerber M, McCullough KC, Summerfield A.** 2006. Plasmacytoid dendritic cell activation by foot-and-mouth disease virus requires immune complexes. Eur. J. Immunol. **36**:1674–1683.
26. **Hardy AW, Graham DR, Shearer GM, Herbeuval JP.** 2007. HIV turns plasmacytoid dendritic cells (pDC) into TRAIL-expressing killer pDC and down-regulates HIV coreceptors by Toll-like receptor 7-induced IFN-alpha. Proc. Natl. Acad. Sci. U. S. A. **104**:17453–17458.
27. **Hemati B, et al.** 2009. Bluetongue virus targets conventional dendritic cells in skin lymph. J. Virol. **83**:8789–8799.
28. **Hervas-Stubbs S, Rueda P, Lopez L, Leclerc C.** 2007. Insect baculoviruses strongly potentiate adaptive immune responses by inducing type I interferon. J. Immunol. **178**:2361–2369.
29. **Hornung V, et al.** 2005. Sequence-specific potent induction of IFN-alpha by short interfering RNA in plasmacytoid dendritic cells through TLR7. Nat. Med. **11**:263–270.
30. **Hornung V, et al.** 2004. Replication-dependent potent IFN-alpha induction in human plasmacytoid dendritic cells by a single-stranded RNA virus. J. Immunol. **173**:5935–5943.
31. **Ingrand S, et al.** 2007. The oxindole/imidazole derivative C16 reduces in vivo brain PKR activation. FEBS Lett. **581**:4473–4478.
32. **Ito M, et al.** 2011. Differential regulation of CIDEA and CIDEC expres-

sion by insulin via Akt1/2- and JNK2-dependent pathways in human adipocytes. J. Lipid Res. **52**:1450–1460.
33. **Jammi NV, Whitby LR, Beal PA.** 2003. Small molecule inhibitors of the RNA-dependent protein kinase. Biochem. Biophys. Res. Commun. **308**: 50–57.
34. **Johansson C, et al.** 2007. Type I interferons produced by hematopoietic cells protect mice against lethal infection by mammalian reovirus. J. Exp. Med. **204**:1349–1358.
35. **Kato H, et al.** 2005. Cell type-specific involvement of RIG-I in antiviral response. Immunity **23**:19–28.
36. **Kim T, et al.** 2010. Aspartate-glutamate-alanine-histidine box motif (DEAH)/RNA helicase A helicases sense microbial DNA in human plasmacytoid dendritic cells. Proc. Natl. Acad. Sci. U. S. A. **107**:15181–15186.
37. **Kumar A, Haque J, Lacoste J, Hiscott J, Williams BR.** 1994. Double-stranded RNA-dependent protein kinase activates transcription factor NF-kappa B by phosphorylating I kappa B. Proc. Natl. Acad. Sci. U. S. A. **91**:6288–6292.
38. **Kumar A, et al.** 1997. Deficient cytokine signaling in mouse embryo fibroblasts with a targeted deletion in the PKR gene: role of IRF-1 and NF-kappaB. EMBO J. **16**:406–416.
39. **Le Bon A, et al.** 2003. Cross-priming of CD8+ T cells stimulated by virus-induced type I interferon. Nat. Immunol. **4**:1009–1015.
40. **Li X, et al.** 2009. The RIG-I-like receptor LGP2 recognizes the termini of double-stranded RNA. J. Biol. Chem. **284**:13881–13891.
41. **Litinskiy MB, et al.** 2002. DCs induce CD40-independent immunoglobulin class switching through BLyS and APRIL. Nat. Immunol. **3**:822–829.
42. **Liu YJ.** 2005. IPC: professional type 1 interferon-producing cells and plasmacytoid dendritic cell precursors. Annu. Rev. Immunol. **23**:275–306.
43. **Loiarro M, et al.** 2005. Peptide-mediated interference of TIR domain dimerization in MyD88 inhibits interleukin-1-dependent activation of NF-{kappa}B. J. Biol. Chem. **280**:15809–15814.
44. **MacLachlan NJ, et al.** 1994. Detection of bluetongue virus in the blood of inoculated calves: comparison of virus isolation, PCR assay, and in vitro feeding of Culicoides variipennis. Arch. Virol. **136**:1–8.
45. **Melino M, Hii CS, McColl SR, Ferrante A.** 2008. The effect of the JNK inhibitor, JIP peptide, on human T lymphocyte proliferation and cytokine production. J. Immunol. **181**:7300–7306.
46. **Mertens PP, Burroughs JN, Anderson J.** 1987. Purification and properties of virus particles, infectious subviral particles, and cores of bluetongue virus serotypes 1 and 4. Virology **157**:375–386.
47. **Mesa MC, Rodriguez LS, Franco MA, Angel J.** 2007. Interaction of rotavirus with human peripheral blood mononuclear cells: plasmacytoid dendritic cells play a role in stimulating memory rotavirus specific T cells in vitro. Virology **366**:174–184.
48. **Mittag D, et al.** 2011. Human dendritic cell subsets from spleen and blood are similar in phenotype and function but modified by donor health status. J. Immunol. **186**:6207–6217.
49. **Moulin V, et al.** 2012. Clinical disease in sheep caused by bluetongue virus serotype 8, and prevention by an inactivated vaccine. Vaccine **30**:2228–2235.
50. **Nakayama Y, et al.** 2010. Role of PKR and Type I IFNs in viral control during primary and secondary infection. PLoS Pathog. **6**:e1000966.
51. **Oh JZ, Kurche JS, Burchill MA, Kedl RM.** 2011. TLR7 enables cross-presentation by multiple dendritic cell subsets through a type I IFN-dependent pathway. Blood **118**:3028–3038.
52. **Pascale F, et al.** 2008. Plasmacytoid dendritic cells migrate in afferent skin lymph. J. Immunol. **180**:5963–5972.
53. **Perez de Diego AC, et al.** 2011. Characterization of protection afforded by a bivalent virus-like particle vaccine against bluetongue virus serotypes 1 and 4 in sheep. PLoS One **6**:e26666.
54. **Reizis B, Colonna M, Trinchieri G, Barrat F, Gilliet M.** 2011. Plasmacytoid dendritic cells: one-trick ponies or workhorses of the immune system? Nat. Rev. Immunol. **11**:558–565.
55. **Robbins SH, et al.** 2008. Novel insights into the relationships between dendritic cell subsets in human and mouse revealed by genome-wide expression profiling. Genome Biol. **9**:R17.
56. **Schulz O, et al.** 2010. Protein kinase R contributes to immunity against specific viruses by regulating interferon mRNA integrity. Cell Host Microbe **7**:354–361.
57. **Schwartz-Cornil I, Epardaud M, Bonneau M.** 2006. Cervical duct cannulation in sheep for collection of afferent lymph dendritic cells from head tissues. Nat. Protoc. **1**:874–879.
58. **Schwartz-Cornil I, et al.** 2008. Bluetongue virus: virology, pathogenesis and immunity. Vet. Res. **39**:46.
59. **Scott I.** 2010. The role of mitochondria in the mammalian antiviral defense system. Mitochondrion. **10**:316–320.
60. **Sen A, Pruijssers AJ, Dermody TS, Garcia-Sastre A, Greenberg HB.** 2011. The early interferon response to rotavirus is regulated by PKR and depends on MAVS/IPS-1, RIG-I, MDA-5, and IRF3. J. Virol. **85**:3717–3732.
61. **Skountzou I, Quan FS, Jacob J, Compans RW, Kang SM.** 2006. Transcutaneous immunization with inactivated influenza virus induces protective immune responses. Vaccine **24**:6110–6119.
62. **Stewart ME, Roy P.** 2010. Role of cellular caspases, nuclear factor-kappa B and interferon regulatory factor in bluetongue virus infection and cell fate. Virol. J. **7**:362.
63. **Sun Q, et al.** 2006. The specific and essential role of MAVS in antiviral innate immune responses. Immunity **24**:633–642.
64. **Sutton KM, et al.** 2007. Selective inhibition of MEK1/2 reveals a differential requirement for ERK1/2 signalling in the regulation of HIF-1 in response to hypoxia and IGF-1. Oncogene **26**:3920–3929.
65. **Swiecki M, et al.** 2011. Type I interferon negatively controls plasmacytoid dendritic cell numbers in vivo. J. Exp. Med. **208**:2367–2374.
66. **Thomis DC, Samuel CE.** 1992. Mechanism of interferon action: autoregulation of RNA-dependent P1/eIF-2 alpha protein kinase (PKR) expression in transfected mammalian cells. Proc. Natl. Acad. Sci. U. S. A. **89**: 10837–10841.
67. **Yoneyama M, et al.** 2005. Shared and unique functions of the DExD/H-box helicases RIG-I, MDA5, and LGP2 in antiviral innate immunity. J. Immunol. **175**:2851–2858.
68. **Yoneyama M, et al.** 2004. The RNA helicase RIG-I has an essential function in double-stranded RNA-induced innate antiviral responses. Nat. Immunol. **5**:730–737.
69. **Zhang Z, et al.** 2011. DDX1, DDX21, and DHX36 helicases form a complex with the adaptor molecule TRIF to sense dsRNA in dendritic cells. Immunity **34**:866–878.